Human Defensins Facilitate Local Unfolding of Thermodynamically Unstable Regions of Bacterial Protein Toxins

Elena Kudryashova,[1] Royston Quintyn,[1] Stephanie Seveau,[2,3] Wuyuan Lu,[4] Vicki H. Wysocki,[1] and Dmitri S. Kudryashov[1,*]
[1]Department of Chemistry and Biochemistry
[2]Department of Microbiology
[3]Department of Microbial Infection and Immunity
The Ohio State University, Columbus, OH 43210, USA
[4]Institute of Human Virology and Department of Biochemistry and Molecular Biology, University of Maryland School of Medicine, Baltimore, MD 21201, USA
*Correspondence: kudryashov.1@osu.edu
http://dx.doi.org/10.1016/j.immuni.2014.10.018

SUMMARY

Defensins are short cationic, amphiphilic, cysteine-rich peptides that constitute the front-line immune defense against various pathogens. In addition to exerting direct antibacterial activities, defensins inactivate several classes of unrelated bacterial exotoxins. To date, no coherent mechanism has been proposed to explain defensins' enigmatic efficiency toward various toxins. In this study, we showed that binding of neutrophil α-defensin HNP1 to affected bacterial toxins caused their local unfolding, potentiated their thermal melting and precipitation, exposed new regions for proteolysis, and increased susceptibility to collisional quenchers without causing similar effects on tested mammalian structural and enzymatic proteins. Enteric α-defensin HD5 and β-defensin hBD2 shared similar toxin-unfolding effects with HNP1, albeit to different degrees. We propose that protein susceptibility to inactivation by defensins is contingent to their thermolability and conformational plasticity and that defensin-induced unfolding is a key element in the general mechanism of toxin inactivation by human defensins.

INTRODUCTION

Human defensins are short cationic immune peptides with a remarkably broad repertoire of antimicrobial activities (Zhao and Lu, 2014). Defensins are major contributors to neutralization of pathogenic microbial flora at the mucosal surfaces and in inflammation areas that act by modulating the activity of immune cells and by exhibiting direct antimicrobial activities. Defensins not only disorganize bacterial cell membranes (Madison et al., 2007; Zhang et al., 2010) and create trapping nanonets around bacteria (Chu et al., 2012) but also inactivate bacterial toxins and viral proteins while showing little effect on the overwhelming majority of the host's proteins. This selectivity of defensins

against various unrelated toxins is not well understood, nor has a coherent hypothesis been proposed to explain this selectivity.

The largest family of toxins known to be inhibited by defensins is pore-forming cholesterol-dependent cytolysins (CDCs), which are major virulence factors produced by many Gram-positive pathogens. They include listeriolysin O (LLO) from *Listeria monocytogenes*, anthrolysin O (ALO) from *Bacillus anthracis*, and pneumolysin (PLY) from *Streptococcus pneumoniae* (Lehrer et al., 2009). Defensins also inhibit diverse enzymatic toxins, such as the binary anthrax lethal toxin (Kim et al., 2005), *Corynebacterium diphtheriae* diphtheria toxin (Kim et al., 2006), *Pseudomonas aeruginosa* exotoxin A (Kim et al., 2006), *Clostridium difficile* toxin B (TcdB; Giesemann et al., 2008), *Staphylococcus aureus* staphylokinase (Bokarewa and Tarkowski, 2004), and others (Castagnini et al., 2012; Hooven et al., 2012). Notably, bacterial toxins represent a variety of enzymatic and structural classes of proteins and therefore cannot be selected by defensins solely on the basis of their specific activity or structure. The observed selectivity toward bacterial toxins implies that many seemingly unrelated toxins share some common features that separate them from the majority of other proteins. Undoubtedly, these elusive toxin-specific traits would be relinquished by bacteria for the sake of being indistinguishable from the host proteins if this didn't detrimentally alter their ability to function as toxins.

We speculate that the elusive property shared by many bacterial toxins is their thermodynamic instability, which is tightly linked to a conformational plasticity indispensable for the formation of a membrane pore (e.g., by CDCs and *B. anthracis* protective antigen) for passing through a narrow pore (e.g., *B. anthracis* lethal factor) or for both (e.g., diphtheria toxin and TcdB). If the above speculations are correct, we should be able to predict a susceptibility of novel toxins, which are not yet recognized as defensin targets, on the basis of their thermodynamic properties. To test this hypothesis, we focused on the effector domains of *Vibrio cholerae* multifunctional autoprocessing repeats-in-toxin (MARTX) toxin (Satchell, 2011) given that they have been recently shown to be thermodynamically unstable (Kudryashova et al., 2014). Similarly to many exotoxins, MARTX effector domains have to cross a pore (formed by the toxin's N- and C-terminal glycine-rich repeats) to reach the cytoplasmic domain of a host cell. In this study, we show that at least some MARTX effector

CrossMark
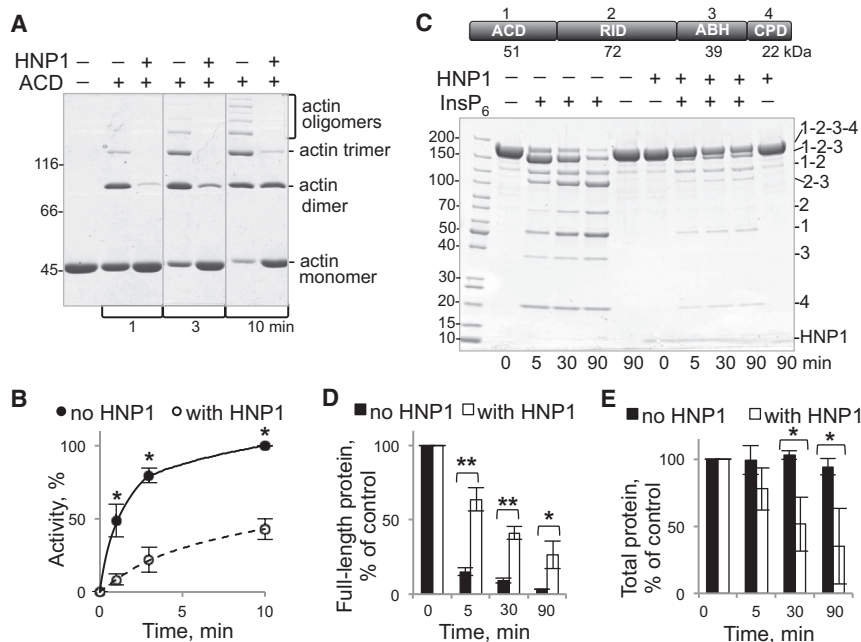
Figure 1. HNP1 Neutralizes the Actin Cross-linking and Autoprocessing Activities of MARTX$_{Vc}$ Toxin

(A) Crosslinking of actin (10 μM) by ACD$_{Vc}$ (50 nM) was conducted in the absence and presence of HNP1 (250 nM) for 1, 3, or 10 min and resolved on 7.5% SDS gels.

(B) Effects of HNP1 on the actin crosslinking activity of ACD$_{Vc}$.

(C) Autocleavage of 4dMARTX (3 μM) with or without HNP1 (36 μM) was activated by the addition of InsP$_6$ and was monitored by electrophoresis on 4%–15% gradient SDS gels. Numbers on the right represent the domains of 4dMARTX as indicated on the scheme given above the gel.

(D) The amount of full-length 4dMARTX (180 kDa band) was quantified in each lane and expressed as a percentage of the initial amount of 4dMARTX before activation.

(E) The amount of total protein was quantified as a sum of all bands in a lane.

Error bars represent SEM, n = 4 experiments, *p < 0.05. See also Figure S1.

domains are efficiently inactivated by human defensin HNP1 (neutrophil defensin 1) under physiological salt, serum, and protein concentrations. Moreover, using the MARTX effector domains and toxins that have been previously recognized as targets for human defensins, we demonstrate that HNP1 and other defensins promote exposure of toxins' hydrophobic interior to ultimately result in their instability, increased susceptibility to proteolysis, precipitation, and functional inactivation. In striking contrast, all tested eukaryotic enzymes and structural proteins were not destabilized by HNP1.

RESULTS

HNP1 Inhibits Proteolytic Autoprocessing of MARTX Toxin and Activity of Its Actin Crosslinking Domain

Recently, we showed that the majority of MARTX effector domains from *V. cholerae* and *Aeromonas hydrophila* are thermodynamically unstable (Kudryashova et al., 2014). To test whether the inhibitory activity of human α-defensin HNP1 extends to MARTX$_{Vc}$ toxin, we assessed its effects on autoprocessing activity of MARTX cysteine protease domain (CPD$_{Vc}$; Prochazkova et al., 2009; Shen et al., 2009) and catalytic activity of the actin crosslinking domain (ACD$_{Vc}$; Kudryashov et al., 2008; Kudryashova et al., 2012). In the presence of HNP1, the initial reaction rate of actin crosslinking by ACD$_{Vc}$ was inhibited by 5.8 ± 1.2-fold, as monitored by reduced accumulation of covalently crosslinked actin species (Figures 1A and 1B). Notably, specific activities of three tested mammalian enzymes (DNase I, catalase, and chymotrypsin) were not altered by HNP1 under similar conditions (Figure S1, available online).

Next, the proteolytic autoprocessing of a recombinant construct containing all four MARTX$_{Vc}$ domains fused together in their natural orientation (4dMARTX$_{Vc}$) was initiated by an activator of CPD: inositol hexakisphosphate (InsP$_6$; Figure 1C). In the absence of HNP1, activated CPD cleaved at the well-defined in-

terdomain linker regions connecting the MARTX$_{Vc}$ effector domains in accordance with previous reports (Prochazkova et al., 2009; Shen et al., 2009). Addition of HNP1 changed the character of the cleavage (1) by causing apparent inhibition of the autoprocessing, as evidenced by a reduced cleavage rate of the full-length 4dMARTX band (Figure 1D), and (2) by reducing the amount of total protein detectable on the gel (determined as the sum of all bands in a lane; Figure 1E). This protein loss occurred only upon CPD activation by InsP$_6$ and thus cannot be a result of unaccounted precipitation (Figure 1C). Because CPD cleaves the exposed Leu residues with low specificity for the adjacent amino acid content (Shen et al., 2009), we hypothesized that the reduction of total protein amount would result from cleavage at additional Leu residues originally buried in the native protein conformation and therefore inaccessible for cleavage by CPD. Exposure of additional cleavage sites would suggest that HNP1 promotes toxin unfolding or misfolding and thus creates conditions for the production of a highly heterogeneous population of randomly fragmented polypeptides that are spread, and therefore undetectable, on the gel.

Limited Proteolysis Suggests Unfolding of Susceptible Toxins in the Presence of HNP1

We tested whether the ability of HNP1 to promote proteolytic degradation extends to other toxins and different proteases. Limited proteolysis is commonly used for identifying sites of high flexibility and/or local unfolding as revealed by higher susceptibility of these regions to proteolytic cleavage (Fontana et al., 2004). Using chymotrypsin and thermolysin, two proteases that cleave at hydrophobic residues, we observed that the band corresponding to the full-length ACD$_{Vc}$ was partially protected by HNP1 (Figure 2A). Given that chymotrypsin activity was preserved in the presence of HNP1 (Figure S1C), this protection suggests that the fully folded state of the toxin might be stabilized by the defensin or, alternatively, protected as a result of
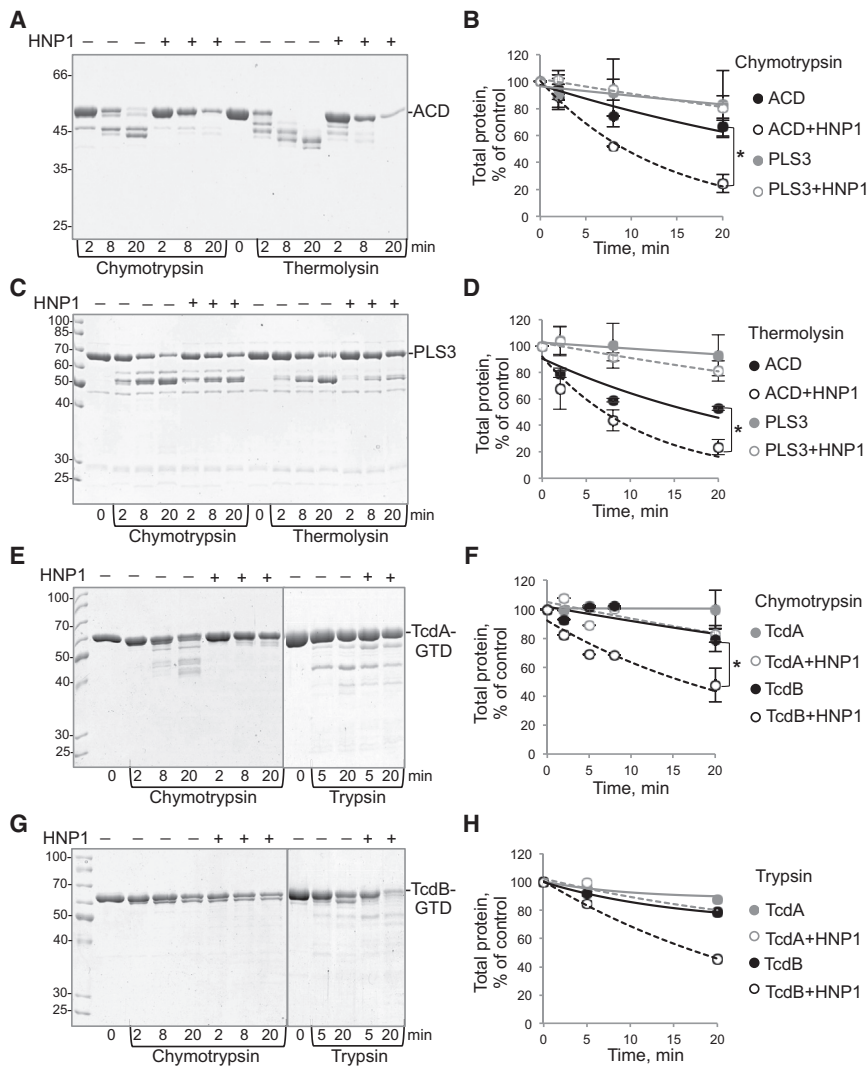
Figure 2. Limited Proteolysis Suggests HNP1-Promoted Unfolding of Susceptible Toxins, but Not Host Structural Proteins

(A, C, E, and G) Proteolytic products of ACD_{Vc} (5 μM, A), PLS3 (5 μM, C), TcdA-GTD (5 μM, E), and TcdB-GTD (5 μM, G) with or without HNP1 (15 μM) were resolved on 10% SDS gels. Usage of proteases and incubation times are indicated in the figure.

(B, D, F, and H) The amount of total protein was quantified as the sum of all bands in a gel lane. Error bars represent SEM, n = 2 experiments, *p < 0.05. Chymotrypsin (B) and thermolysin (D) digestion of ACD (black lines) and PLS3 (gray lines) is shown, and chymotrypsin (F) and trypsin (H) digestion of TcdB (black lines) and TcdA (gray lines) is shown. Closed circles indicate no HNP1, and open circles indicate the presence of HNP1. See also Figure S2.

the catalytic glucosyltransferase domain (GTD) of TcdB, but not that of TcdA, was promoted by HNP1, resulting in the reduction of the total TcdB-GTD content and only minimal impact on the total protein content of TcdA-GTD (Figures 2E–2H). All together, these results support the hypothesis that HNP1 facilitates unfolding of susceptible toxins and that the observed elevated level of proteolytic susceptibility contributes to the mechanism of toxin inactivation by defensins.

Collisional Quenching Reveals Destabilization of Susceptible Toxins by HNP1

Intrinsic Trp fluorescence is a valuable noninvasive reporter of conformational changes in a protein. Particularly, higher accessibility of Trp residues to collisional quenchers (e.g., acrylamide; Eftink and Ghiron, 1976) is indicative of a higher degree of protein unfolding. At a 3:1 molar ratio to proteins, the Trp fluorescence intensity of HNP1 constituted 5%–6% of the fluorescence signal of the examined proteins (Figure S3). HNP1 fluorescence was only mildly (~20%) increased in the presence of the MARTX$_{Vc}$ α/β-hydrolase (ABH$_{Vc}$) effector domain, which naturally does not have Trp residues, and was not increased in the presence of a Trp-null mutant of human profilin 1 (Figures S3A and S3B). Acrylamide quenching of HNP1 was unaffected by the addition of Trp-lacking profilin 1 or was even inhibited in the presence of ABH$_{Vc}$ (Figure 3A). Therefore, a single Trp of HNP1 does not significantly contribute to the fluorescence and quenching of the defensin-toxin complexes by acrylamide. We found that collisional quenching of Trp fluorescence of actin, PLS3, and TcdA-GTD was not affected by HNP1 (Figures 3B, 3C, and 3E; Table S1). In contrast, acrylamide quenching of toxins susceptible to HNP1 (ACD$_{Vc}$ and TcdB-GTD) was increased in the presence of HNP1 (by 63% and 31%, respectively), suggesting that at least some of the eight tryptophans of ACD$_{Vc}$ and the five

protein precipitation (Figure S2A). At the same time, proteolytic fragments of ACD$_{Vc}$ were prominent in the absence of HNP1 but undetectable in the presence of the defensin (Figure 2A). Accordingly, total protein content of ACD$_{Vc}$ was strongly reduced upon limited proteolysis in the presence of HNP1 (Figures 2A, 2B, and 2D). Immunoblot with polyclonal anti-ACD antibody (Cordero et al., 2006) revealed otherwise invisible bands of lower molecular masses in the presence of, but not in the absence of, HNP1 (Figure S2B). This confirms that the apparent disappearance of total ACD$_{Vc}$ content stems from cleavage at additional sites otherwise inaccessible for proteolysis. The addition of HNP1 to mammalian protein plastin 3 (PLS3; Figures 2B–2D) or actin (Figure S2C) also slowed down protein cleavage but neither changed the pattern of the obtained cleavage products nor substantially affected the total protein content.

HNP1 is known to inhibit cytotoxicity inflicted by *C. difficile* TcdB, but not by a homologous toxin A (TcdA) (Giesemann et al., 2008). If the observed destabilization and increased proteolytic susceptibility reflect the general mechanism of antitoxin activity of defensins, then only the cleavage of TcdB, but not of TcdA, would be potentiated. Indeed, the enzymatic digestion of

Figure 3. Collisional Quenching Suggests Greater Exposure of Trp Residues of Susceptible Toxins in the Presence of HNP1

Trp fluorescence intensity of proteins (2 μM) with or without HNP1 (6 μM) was monitored after the addition of increasing concentrations of acrylamide. Stern-Volmer plots represent the ratios of the fluorescence intensity in the absence of quencher (F_o) to the intensity in the presence of quencher (F); the ratios are plotted against quencher (acrylamide) concentration. Stern-Volmer plots are shown for HNP1 (A), actin (B), PLS3 (C), ACD_{Vc} (D), TcdA-GTD (E), and TcdB-GTD (F). Error bars represent SEM, n = 3 experiments, *p < 0.05. See also Figure S3 and Table S1.

tryptophans of TcdB-GTD were more exposed to solvent in the presence of HNP1 (Figures 3D and 3F; Table S1).

Ion Mobility Mass Spectrometry Reveals Conformational Changes in Toxins upon HNP1 Binding

Coupling of ion mobility (IM) to mass spectrometry (MS) enables measuring the stoichiometry of protein-ligand interactions (Yin et al., 2008) and probing interaction-mediated conformational changes (Niu et al., 2013). The latter is deduced from collisional cross section (CCS) values for complexes and individual interacting partners upon their surface-induced dissociation (SID) or collision-induced dissociation. However, precipitation observed upon addition of HNP1 to all tested toxins in conventional MS buffers, such as ammonium acetate, prevented our attempts to analyze toxin-HNP1 complexes by IM-MS. We hypothesized that the precipitation was caused by an HNP1-promoted exposure of the toxin's hydrophobic residues. To prevent precipitation, we applied a nonionic detergent, n-dodecyl β-D-maltoside (DDM), which is known to stabilize hydrophobic surfaces of membrane-protein complexes via Van der Waals interactions in the gas phase (Barrera et al., 2008). We used very gentle source conditions to remove DDM molecules from protein-containing micelles upon their transfer to the gas phase. Relatively broad protein peaks detected by MS analysis (Figures S4A and S4B) suggest that a small subset of DDM molecules remained associated with the proteins sequestered either by natively occurring hydrophobic cavities on protein surfaces or by hydrophobic regions exposed as a result of the binding of defensin. Also, the experimental mass of the peaks in the presence of HNP1 was significantly larger than their predicted mass for both ACD_{Vc} and *B. anthracis* protective antigen (PA) toxins, but

not for actin (Table S2). We speculate that this larger deviation in the mass observed for the ACD_{Vc} and PA toxins was due to the HNP1-promoted exposure of larger hydrophobic areas involved in DDM binding. Accordingly, stripping off the remaining DDM by selecting a specific charge state for tandem MS analysis did not substantially affect the difference observed between the experimental and predicted masses for actin and actin-defensin complexes but strongly narrowed it for both ACD_{Vc} and PA in the presence of HNP1 (Figure S4C and S4D; Table S2).

To evaluate structural perturbations caused by HNP1 binding to proteins, we compared the CCS values determined in IM-MS experiments with those theoretically estimated by MOBCAL (Figure 4; Supplemental Experimental Procedures). The calculations were conducted with an HNP1 monomer positioned to cause the smallest and the largest possible impacts on the CCS value under the assumption of rigid body interactions between the partners (Figure 4A). The experimentally determined percentage change in CCS observed for the actin-defensin complex (4.9% ± 0.9%) fell well within the range obtained from MOBCAL calculations (0.8%–8.7%), suggesting no significant conformational changes in actin in response to HNP1 binding (Figures 4A and 4B). In striking contrast, for ACD_{Vc}, the experimentally determined change in CCS due to the presence of defensin (10.4% ± 0.8%) was nearly 2-fold greater than the maximum value of 5.7% obtained from MOBCAL calculations (Figures 4A and 4B). Because the fully unfolded ACD_{Vc} state determined in the presence of 50% acetonitrile corresponds to a 41.7% ± 0.2% increase in CCS (data not shown), we conclude that HNP1 binding causes ACD_{Vc} deformation that can be best described as partial, or local, unfolding. Although the percentage change in CCS due to the presence of defensin in PA was smaller (6.1% ± 0.7%), it was still above the theoretically modeled maximum range for CCS values (0.5%–4.6%; Figures 4A and 4B).

Activation of both actin and the actin-defensin complex in SID experiments with acceleration voltage of 100V revealed one major conformational state and a slightly larger CCS value for the actin-defensin complex (Figure 4C). In agreement with low thermodynamic stability of ACD_{Vc} (Kudryashova et al., 2014),
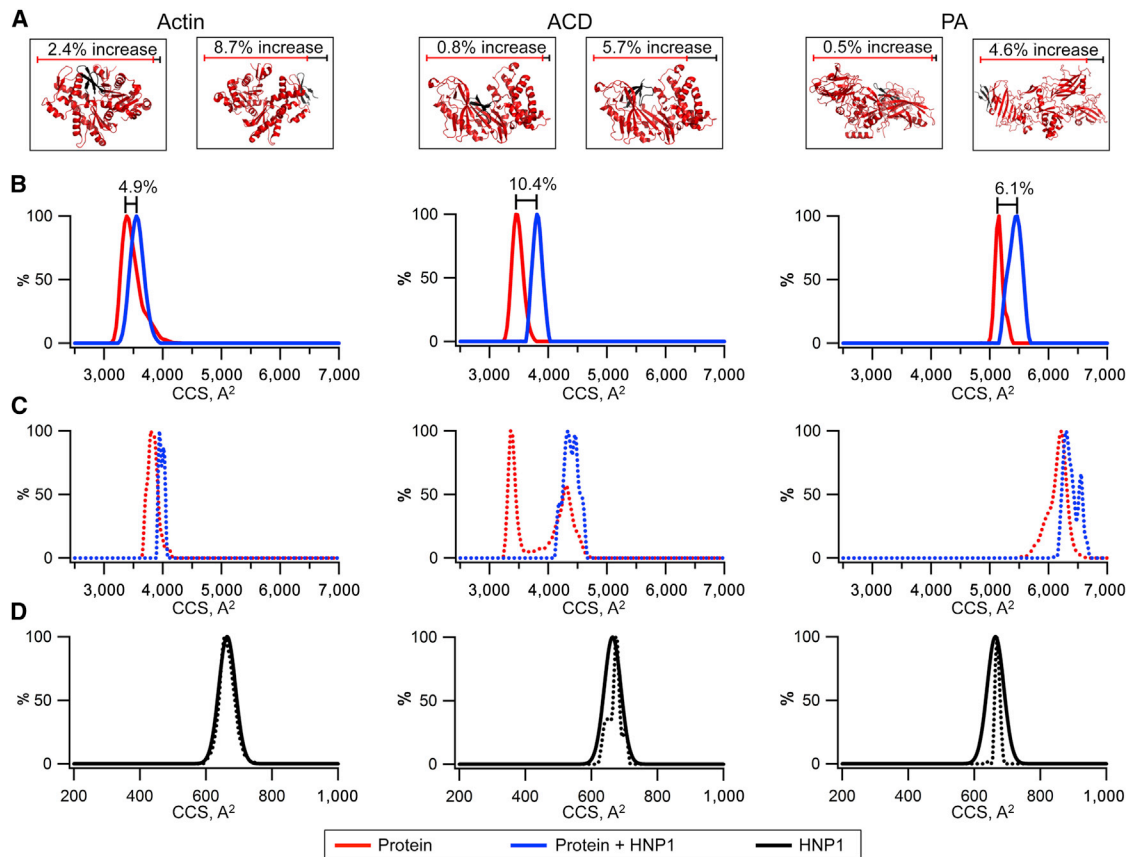
Figure 4. The Effect of HNP1 on CCS Values of Various Proteins

Left panels show actin, middle panels show ACD_{Vc}, and right panels show PA. The concentration of all proteins is 10 μM, and that of HNP1 is 30 μM.

(A) The predicted ranges of CCS value changes for actin, ACD_{Vc}, and PA in the presence of HNP1.

(B) The MS-determined CCS value for protein (red) and the protein-defensin complex (blue).

(C) The CCS value determined from an SID acceleration voltage of 100V for protein (red) and the protein-defensin complex (blue).

(D) The CCS value determined from an SID acceleration voltage of 100V for HNP1 that was sprayed from solution (black line) and HNP1 that was removed from protein (black dots).

See also Figure S4 and Table S2.

the toxin's SID activation yielded two distinct states—a "native" state with a CCS value similar to that found in MS analysis and an "unfolded" state with a significantly higher CCS value (Figure 4C). Activation of the ACD-defensin complex produced only the unfolded state. SID activation of the PA-defensin complex showed the presence of partially unfolded and deeply unfolded states, whereas the activation of PA alone yielded only a relatively more stable partially unfolded state (Figure 4C). Therefore, HNP1 destabilizes both ACD_{Vc} and PA, albeit to a different extent, but does not affect the stability of actin. Also, no significant difference in CCS values was observed between free activated defensin and HNP1 removed upon activation of the protein-defensin complex (Figure 4D), suggesting that the detected conformational changes occurred within the toxins and not the defensin.

Both Tertiary and Secondary Structures of ACD_{Vc} Are Destabilized by HNP1

We examined the effects of HNP1 on the unfolding of ACD_{Vc} by circular dichroism (CD) and differential scanning fluorimetry

(DSF) (Senisterra and Finerty, 2009). CD revealed that the effects of HNP1 on the secondary structure of ACD_{Vc} (Figure 5A) were similar to the destabilizing effects of guanidine hydrochloride (Gdn-HCl; Figure 5B). A CD spectrum of HNP1 was not affected by temperatures up to 70°C (Figure 5C), whereas the apparent melting temperature of the secondary structure of ACD_{Vc} was reduced by ~10°C in the presence of the defensin (Figure 5D).

The DSF approach allows for monitoring changes in protein tertiary structure by an increase in fluorescence of an environmentally sensitive dye (e.g., SYPRO Orange [SO]) upon its interaction with denaturation-exposed hydrophobic residues of a target protein. The addition of 2- to 3-fold molar excess of HNP1 over ACD_{Vc} caused a dramatic increase in the fluorescence intensity of the dye at lower temperatures, suggesting that HNP1 promoted thermal unfolding of ACD_{Vc} tertiary structure in a concentration-dependent manner and thus caused toxin denaturation comparable to that caused by 1 M Gdn-HCl (Figures 5E and 5F). A similar DSF melting profile was observed for serum albumin, a protein with high surface hydrophobicity (Figure S5A).
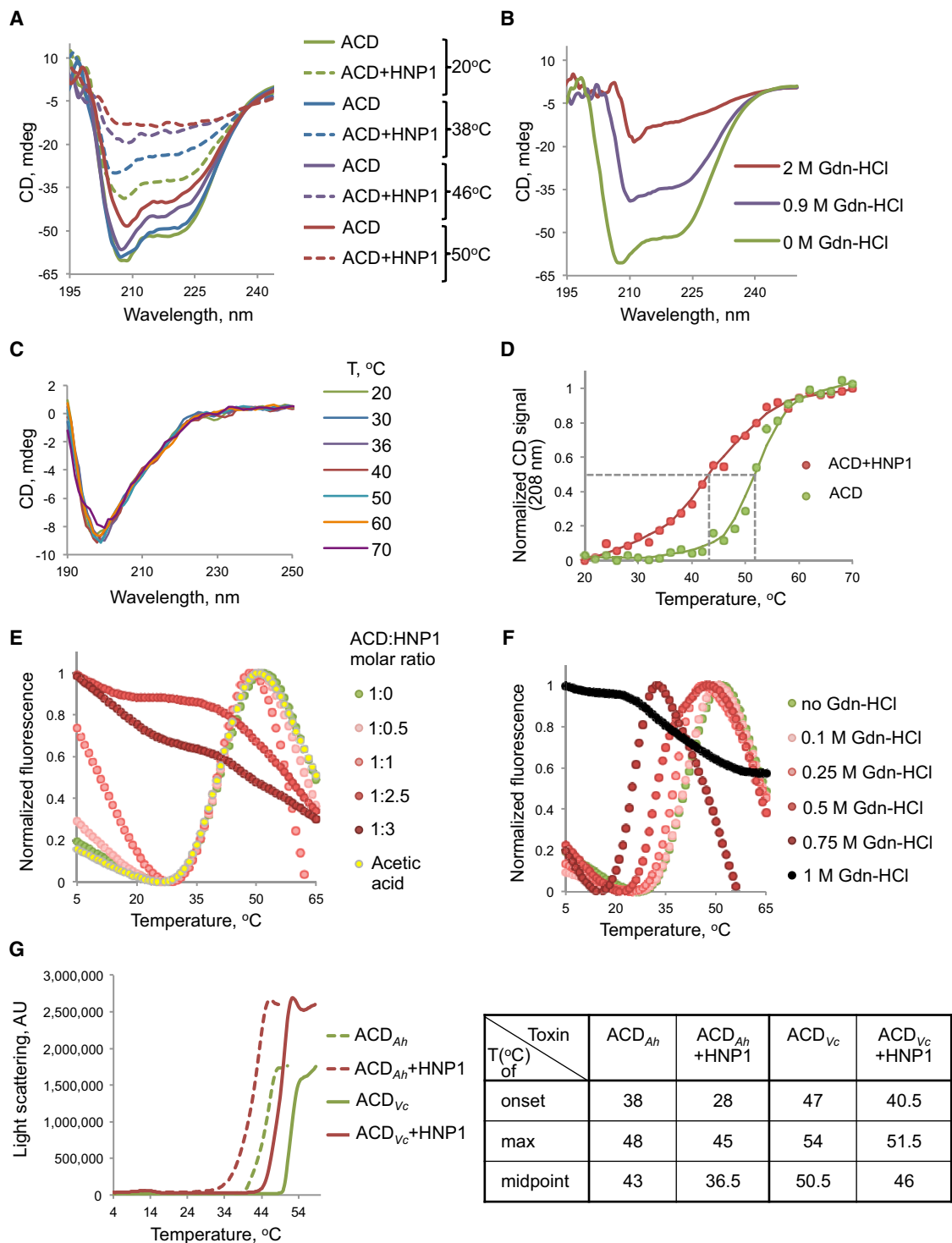
Figure 5. Tertiary and Secondary Structures of ACD$_{Vc}$ Are Destabilized by HNP1

(A) Far-UV CD spectra of ACD$_{Vc}$ (0.5 mg/ml; 10 μM) in the absence (solid lines) or presence (dotted lines) of 30 μM HNP1 at four different temperatures.

(B) Far-UV CD spectra of 10 μM ACD$_{Vc}$ denatured by various Gdn-HCl concentrations.

(C) Far-UV CD spectra of 30 μM HNP1 at different temperatures.

(D) Thermal denaturation of ACD$_{Vc}$ (0.5 mg/ml; 10 μM) in the absence (green) or presence (red) of HNP1 (30 μM) as assessed by far-UV CD. Positions of the apparent melting temperatures are shown by dotted lines.

(E) Thermal denaturation of 10 μM ACD$_{Vc}$ in the presence of increasing concentrations of HNP1 (up to 3-fold molar excess) as assessed by DSF. "Acetic acid" represents a control to account for the effect of the solvent (0.01% acetic acid) added with HNP1.

(legend continued on next page)

Precipitation of bacterial toxins by defensins has been attributed to tethering of a toxin by defensin oligomers (Lehrer et al., 2009). To rule out the possibility that trapping of the environmental dye by large protein aggregates can cause the observed increase in SO fluorescence, we analyzed unfolding of PLS3-actin bundles large enough to be pelleted under low-speed centrifugation conditions (20 min at 17,000 × g; Figure S5B). SO did not interact with the actin bundles at lower temperatures, suggesting that the dye interaction with HNP1-toxin complexes is mediated by the exposed hydrophobic regions and not by large protein aggregates per se.

Next, we tested whether the ability of HNP1 to promote precipitation is related to the protein's thermodynamic instability. We monitored a temperature-induced precipitation (followed by a raise in light scattering) of two ACD orthologs (*V. cholerae* ACD_{Vc} and *A. hydrophila* ACD_{Ah}) that share 80% sequence similarity but differ significantly in their thermodynamic stability (Kudryashova et al., 2014). We reduced the probability of multivalent tethering of toxin molecules with HNP1 by keeping both components at equimolar concentrations of 2.5 μM. Both toxins precipitated near their secondary-structure melting temperatures, which are significantly higher than temperatures of unfolding of their tertiary-structure elements, confirming our finding that ACD melts via a molten globule state (Kudryashova et al., 2014). The addition of equimolar concentrations of HNP1 lowered precipitation temperatures of ACD_{Vc} and ACD_{Ah} by 4.5°C and 6.5°C, respectively (Figure 5G), in agreement with the proposed ability of defensins to promote unfolding and thus potentiate precipitation of susceptible proteins.

HNP1 Potentiates Thermal Unfolding of Several Major Toxin Family Members, but Not Human Proteins, as Revealed by the DSF Approach

We examined the effects of HNP1 on various toxins, including both those already recognized as targets of defensins (anthrax toxin, TcdB, and CDCs [LLO, ALO, and PLY]) and others (effector domains of the $MARTX_{Vc}$ toxin [ACD_{Vc} and CPD_{Vc}] and $MARTX_{Ah}$ toxin [ACD_{Ah} and CPD_{Ah}], domains with unknown function [ABH_{Vc} and PMT_{Ah}], and all four effector domains expressed as a single polypeptide chain [$4dMARTX_{Vc}$]), for which such effects have not been reported so far. Notably, HNP1 strongly promoted denaturation of all but two tested toxins—TcdA-GTD and PLY (Figure 6; Figure S6). Both toxins showed only slight or no destabilization by HNP1, confirming their relative resistance to defensins (Giesemann et al., 2008; Lehrer et al., 2009). In striking contrast, most of the tested mammalian structural proteins and enzymes (PLS3, DNase I, creatine kinase, and citrate synthase) were not affected by HNP1, whereas actin, cofilin, and catalase were stabilized by HNP1 (Figure 6; Figure S6).

Toxin Inhibition by HNP1 under Physiological Conditions

Next, we sought to explore the activity of HNP1 under physiologically relevant concentrations of salts, serum, toxins, and HNP1. To this end, we used the delivery machinery of anthrax toxin (protective antigen [PA] and the N terminus of lethal factor [LF_N]) to translocate LF_N-fusion constructs of ACD_{Vc} (Cordero et al., 2006) and RID_{Vc} (Rho inhibitory domain of $MARTX_{Vc}$; Satchell, 2011) across the membrane. We found that as little as 2.5 μM HNP1 was sufficient to confer notable protection of cultured normal intestinal epithelium cells (IEC-18) against nanomolar quantities of LF_NACD or LF_NRID toxins in complex with PA (Figure 7), whereas 10 and 5 μM HNP1 (recapitulating plasma defensin concentrations under severe infection; Panyutich et al., 1993) completely inhibited cell shrinking and/or rounding inflicted by LF_NACD and LF_NRID, respectively, while imposing no cytotoxicity (Figure 7C). The difference in the effective concentrations argues that the inhibitory effects of HNP1 were at least partially mediated through MARTX effector domains (ACD_{Vc} and RID_{Vc}) and not solely through the inhibition of the LF_N and PA components of anthrax toxin. Importantly, in the cellular assays, HNP1 was added only after the toxins were diluted in a serum-containing medium, proving the potency of the defensin under physiological salt and serum concentrations.

The Ability of HNP1 to Destabilize Toxins Is Shared by Other Defensins

We employed DSF and limited proteolysis to test the effects of enteric α-defensin HD5 and β-defensin hBD2 on unfolding of ACD_{Vc} toxin. DSF revealed that all tested defensins destabilized ACD_{Vc}, albeit to a different extent, and that β-defensin hBD2 was the least potent of all four (Figures S7A–S7C). Moreover, physiological salt completely abolished the activity of hBD2 while imposing only marginal and mild effects on the activities of HNP1 and HD5, respectively (Figures S7D–S7F). Additionally, HD5, but not hBD2, demonstrated effects similar to HNP1 effects on the limited proteolysis of ACD_{Vc} (Figures S7G and S7H). These results suggest that unfolding of thermolabile toxins is a general mechanism shared by several defensins.

DISCUSSION

Secretion of defensins is a vital part of an innate humoral immune response and allows neutralization of a broad spectrum of microbial and viral effector proteins before they get a chance to contact host cells. We have demonstrated here that toxins' inactivation by human α-defensin HNP1 is accompanied by destabilization of their secondary and tertiary structures and local unfolding and that these lead to increased solvent exposure of hydrophobic residues. Because none of the tested mammalian proteins were affected by HNP1 in a comparable way, we speculate that defensins take advantage of intrinsic thermodynamic instability of bacterial toxins required to maintain their high structural plasticity. This high structural plasticity is essential for forming pores or passing across the host cell membranes. Thus, pore-forming CDCs (Marriott et al., 2008; Seveau, 2014) undergo dramatic conformational reshaping upon binding to cholesterol on host membranes, culminating in the refolding of critical α helices into β strands for the formation

---

(F) Thermal denaturation of 10 μM ACD_{Vc} in the presence of various Gdn-HCl as assessed by DSF.

(G) Temperature-induced precipitation of 2.5 μM ACD_{Vc} (solid lines) and ACD_{Ah} (dotted lines) as assessed by light scattering (AU, arbitrary unit) in the presence or absence of an equimolar concentration (2.5 μM) of HNP1. The table shows temperatures of the onset, maximum, and midpoint of precipitation.

See also Figure S5.
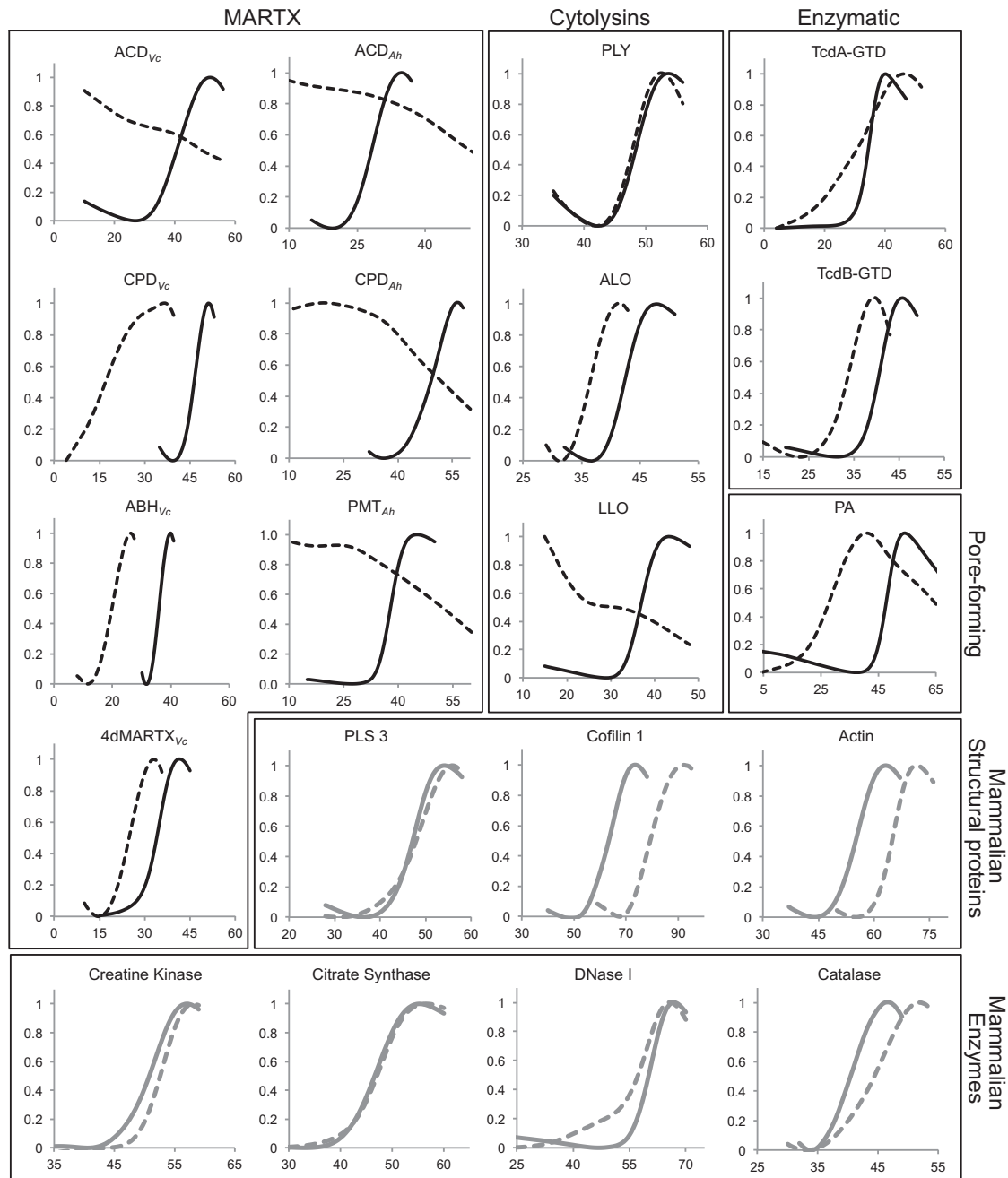
Figure 6. HNP1 Potentiates Thermal Unfolding of Several Major Toxin Family Members, but Not Mammalian Proteins
Thermal unfolding of the domains of MARTX$_{Vc}$ and MARTX$_{Ah}$ toxins (ACD$_{Vc}$, CPD$_{Vc}$, ABH$_{Vc}$, 4dMARTX$_{Vc}$, ACD$_{Ah}$, CPD$_{Ah}$, and PMT$_{Ah}$), enzymatic GTD domains of *C. difficile* TcdA and TcdB, and pore-forming toxins (*B. anthracis* PA and CDCs [PLY, LLO, and ALO]) was monitored by DSF in the absence (solid lines) or presence (dotted lines) of 3-fold molar excess of HNP1. Melting of mammalian structural proteins (PLS3, cofilin 1, and actin) and enzymes (creatine kinase, citrate synthase, DNase I, and catalase) was assessed under identical conditions. Final concentrations of LLO, cofilin, and both CPDs were 20 μM; all other proteins were kept at 10 μM. The fluorescence signals (y axes) were normalized in the transition region (0 = minimum, 1 = maximum) and are plotted against temperature (°C) on the x axes. Non-normalized, raw data are given in Figure S6.

of the β-barrel pore complex (Dunstone and Tweten, 2012). Many membrane-penetrating exotoxins also demonstrate a high degree of instability, which is required for their efficient translocation across the membrane. Thus, effector domains of both anthrax and diphtheria toxins must be unfolded to cross a narrow (∼12Å) pore and reach their cytosolic targets (Montagner et al., 2007; Thoren and Krantz, 2011). Although low-pH conditions and interaction with pore-forming subunits facilitate unfolding (Feld et al., 2012), an effector domains' inherent pliability per se appears to be crucial, given that toxin crosslinking and/or
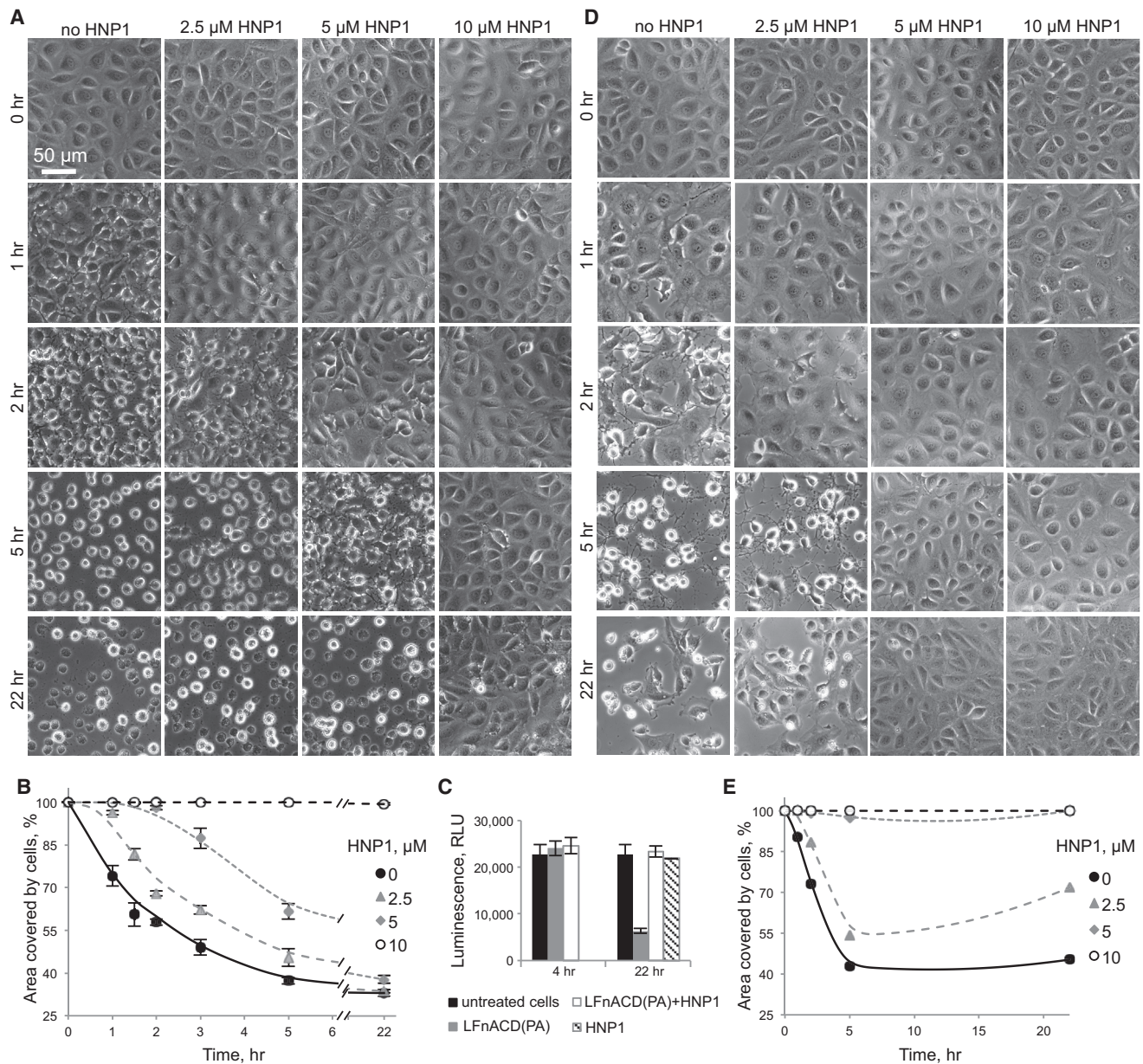
Figure 7. HNP1 Efficiently Inhibits the Effects of Toxins on Cultured Cells in the Presence of Serum

(A and D) IEC-18 cells were treated with 5 nM LF$_N$ACD (A) or LF$_N$RID (D) complexed with 11.5 nM PA in the presence of different concentrations of HNP1 (0–10 μM, as indicated) in complete DMEM with 10% FBS. The scale bar represents 50 μm.

(B and E) The area covered by cells was quantified with NIS Elements software (Nikon) and is plotted against time: LF$_N$ACD treatment (B) and LF$_N$RID treatment (E).

(C) Viability of IEC-18 cells after LF$_N$ACD and HNP1 treatment was assessed with Cell Titer-Glo Luminescent Cell Viability Assay (Promega). RLU, relative luminescence unit.

stabilization can block its passage through the membrane (Wesche et al., 1998).

It is tempting to speculate that the proposed vulnerability of marginally stable proteins might extend well beyond bacterial toxins and include secretion machineries of Gram-positive bacteria (Arnett et al., 2011; Vega and Caparon, 2012), as well as numerous capsid and noncapsid viral proteins (Furci et al., 2007; Gounder et al., 2012). Many viral proteins display loosely packed cores (a hallmark of thermodynamic instability) that provide evolutionary advantage by conferring high interactive promiscuity and high mutational adaptability (Tokuriki et al., 2009; Wylie and Shakhnovich, 2011). Accordingly, more than a dozen viruses are currently recognized as targets of defensins (Wilson et al., 2013). Furthermore, the proposed local unfolding of affected proteins explains many hitherto enigmatic properties of defensins. Thus, it explains the amazing ability of HNP1 to

inhibit multiple steps of HIV-1 entry (Demirkhanyan et al., 2012), given that many viral proteins (particularly those of RNA viruses) possess low thermodynamic stability (Tokuriki et al., 2009; Wylie and Shakhnovich, 2011).

The ability of defensins to oligomerize and thereby create bridges between toxin molecules has been proposed as an essential element of toxin precipitation (Lehrer et al., 2009). Yet, our IM-MS and light-scattering data suggest that binding of a single HNP1 monomer is sufficient to cause partial unfolding of a targeted toxin and facilitate its precipitation. Consequently, it should be considered that precipitation might arise from the defensin-potentiated exposure of otherwise hidden hydrophobic residues of the affected proteins and subsequent self-aggregation due to a hydrophobic effect. Therefore, it is plausible that various mechanisms of toxin inactivation by defensins can be derived from the ability of these peptides to promote local unfolding of the affected toxins. As a result of this unfolding, toxins might become more immunogenic (Kohlgraf et al., 2010), more susceptible to proteolysis (present study), and more prone to aggregation (Lehrer et al., 2009), whether with themselves or with hydrophobic surfaces of serum proteins. The latter is a possible mechanism of inactivation of nanomolar quantities of LF$_N$ACD and LF$_N$RID toxins complexed with PA in the presence of serum when a toxin's concentration (5 nM) is 4 orders of magnitude lower than the serum albumin concentration (~50–80 μM). Moreover, precipitation might not be strictly required for inactivation if HNP1 binds to an active and/or interactive site of a targeted molecule (Furci et al., 2007). This latter possibility should be a common event given that active sites and sites of protein-protein interaction often include loosely packed (partially disordered) regions with highly interactive properties (Flatt et al., 2013; Hsu et al., 2012).

Although our model suggests that thermodynamic instability is the decisive characteristic of protein susceptibility to defensins, other traits must contribute to the selectivity of inactivation. Indeed, despite having a high degree of structural similarity, defensins vary in their ability to neutralize different toxins (Giesemann et al., 2008; Lehrer et al., 2009). Vice versa, highly related toxins can have different susceptibility to inactivation by defensins (e.g., TcdA versus TcdB and PLY versus ALO and LLO). It has been explicitly demonstrated that defensins' cationicity, hydrophobicity, and ability to form dimers and oligomers all contribute, albeit to different degrees, to the specific activity of these peptides (Conibear et al., 2012; Wei et al., 2010; Zhao et al., 2012; Zhao et al., 2013). The detailed mechanisms of protein inactivation could vary in each particular case and would require comprehensive investigation, but we would like to propose here the following unifying model of defensin mechanisms:

1. Defensin dimers, whose hydrophobic surfaces are mainly hidden at the dimerization surface, are attracted to negatively charged regions of a protein via electrostatic interactions. These interactions would be nonspecific and largely transient under physiological salt conditions and would apply to many proteins—both pathogenic and host.
2. Whether or not the electrostatic interactions advance to a new stage will depend on the thermodynamic stability of a targeted protein. For various bacterial toxins and viral proteins, a low thermodynamic stability (a low positive energy change of unfolding) suggests that under the physiological conditions, a detectable population of a protein exists in a partially unfolded state in a dynamic equilibrium with the fully folded state. Thermodynamic instability—together with a tendency of many bacterial toxins to form a molten globule state that is compact enough to protect them from proteolysis and aggregation but is also substantially pliable to provide wanted structural flexibility—is a tentative toxin's "Achilles heel," targeted by defense peptides. We speculate that defensin dimers loosely bound to a surface of such a protein (and therefore present at the surface at a high local concentration) would take advantage of a protein's instability by rearranging hydrophobic interactions from homomolecular (within a dimer) to conceivably more potent heteromolecular (between dissociated defensin monomers and an exposed protein's hydrophobic interior).
3. The strength of this interaction would be defined by how the combination of polar and nonpolar residues on a defensin matches that on the affected protein and might explain differences in susceptibility of otherwise similar proteins to defensin (e.g., TcdB versus TcdA). However, such a rearrangement will not occur with stable proteins, whose hydrophobic residues never (or rarely) get exposed to solution, and thus defensins would only transiently interact with such proteins. Our model calls for the existence of acidic residues in proximity of loosely ordered regions, but given the overall low thermodynamic stability of many bacterial and viral effector proteins, such a combination of properties should be fairly common.
4. As a result of the overall low specificity of these interactions, defensins integrated into disordered regions of thermodynamically unstable proteins would stabilize numerous conformations of partially unfolded proteins with high aggregation propensity.

Although none of the analyzed mammalian proteins from distinct groups (structural proteins and enzymes) were destabilized by HNP1, we concede the possibility that a small fraction of host proteins could also be affected by the defensin but would remain mainly inaccessible because of their intracellular compartmentalization. It is worth noticing, therefore, that selectivity of defensins toward toxins is only relative but is sufficient to bestow protection of the host under conditions of severe infection or even direct injection of lethal toxins (Kim et al., 2005).

To summarize, we propose a unifying working model suggesting that defensins act as selective molecular antichaperones that facilitate local unfolding of (or rather cofolding with) thermodynamically unstable regions of bacterial and viral effector proteins to promote their untimely or unnatural conformational transitions and thus render them prone to aggregation and proteolysis. Therefore, intrinsic structural pliability of membrane-penetrating pathogenic exotoxins might represent the essential element of their functionality and the "Achilles heel" that can be efficiently exploited by human defensins.

EXPERIMENTAL PROCEDURES

Production of Defensins and Proteins

Defensins HNP1, HD5, and hBD2 were prepared by solid-phase peptide synthesis, and the correct folding was ensured as described previously (Wu et al., 2004; Wu et al., 2003a; Wu et al., 2003b). Preparation of all MARTX$_{Vc}$ and

MARTX$_{Ah}$ constructs (Kudryashova et al., 2014), PA (Wesche et al., 1998), and CDCs (LLO, ALO, and PLY; Arnett et al., 2014; Glomski et al., 2002) has been published. TcdA- and TcdB-GTD constructs were expressed in *Bacillus megaterium* cells (provided by Dr. Lacy, Vanderbilt University) and purified as described previously (Chumbler et al., 2012). The LF$_N$ACD expression plasmid was a gift from Dr. Satchell (Northwestern University; Cordero et al., 2006). Preparation of skeletal-muscle actin from rabbit skeletal-muscle acetone powder (Pel-Freez Biologicals; Spudich and Watt, 1971) and purification of recombinant human cofilin 1 (Hawkins et al., 1993) and PLS3 (Lyon et al., 2014) were described previously.

Limited Proteolysis

Five micromolars of ACD$_{Vc}$,TcdA-GTD, TcdB-GTD, PLS3, or actin was preincubated with or without 15 μM HNP1 in either 50 mM HEPES (pH 7.5) or 20 mM TRIS (pH 7.5), 150 mM NaCl, and 5 mM CaCl$_2$ buffer for 15 min and then cleaved by chymotrypsin (1:100 w/w ratio to protein), trypsin (1:100 w/w ratio), or thermolysin (1:200 w/w ratio to protein) at 30°C for the indicated periods of time. Reactions were stopped by the addition of reducing sample buffer supplemented with 2 mM PMSF and 10 mM EDTA, samples were boiled for 5 min, and proteins were resolved on 10% SDS-polyacrylamide gels. See Figures 2 and Figures S2 and S7.

Intrinsic Trp Fluorescence and Collisional Quenching by Acrylamide

Fluorescence-emission spectra of proteins were recorded with the FlouroMax-3 spectrofluorometer (Jobin Yvon Horiba) with an excitation wavelength of 295 nm. Fluorescence-quenching experiments were performed with an excitation wavelength of 295 nm and an emission wavelength corresponding to emission λ$_{max}$ for each protein. Two micromolars of sample protein in PBS with or without 3-fold molar excess of HNP1 was mixed with freshly prepared acrylamide solution in PBS. The data analysis is described in Supplemental Experimental Procedures.

MS

Ten micromolars of sample protein was dialyzed into 100 mM ammonium acetate buffer (pH 7.4) and supplemented with 300 μM DDM and 25 mM triethylammonium acetate. A 3-fold molar excess of HNP1, followed by DDM, was added to the protein. Nano-electrospray ionization MS analysis was conducted on a modified quadrupole IM time-of-flight instrument (SYNAPT G2, Waters) with a customized SID device installed before the IM chamber as previously described (Zhou et al., 2012). See also Supplemental Experimental Procedures.

DSF

Temperature denaturation curves of the proteins diluted in PBS (pH 7.4) to 10–20 μM in the presence of SO dye (Invitrogen) were obtained with the CFX96 Touch Real-Time PCR Detection System (Bio-Rad) as described previously (Kudryashova et al., 2014). See Figures 5 and 6 and Figures S5–S7.

CD

Far-UV CD spectra were collected with the JASCO J-815 CD instrument (JASCO Analytical Instruments) and were analyzed as previously described (Kudryashova et al., 2014).

Cell-Culture Experiments

LF$_N$ACD (Cordero et al., 2006) or LF$_N$RID (created in the present study; see Supplemental Experimental Procedures) was mixed with PA and added to complete Dulbecco's modified Eagle's medium (DMEM) containing 10% fetal bovine serum. Final concentrations of LF$_N$ toxin and PA were 5 and 11.5 nM, respectively. Various concentrations of HNP1 (0–10 μM) were added, and after 20 min incubation at 37°C, the above mixtures were used to replace the medium on the monolayers of IEC-18 cells (ATCC CRL-1589). Phase-contrast microphotographs were taken with the Nikon inverted microscope Eclipse Ti-E and quantified with NIS Elements software (Nikon). All experiments were conducted in triplicates with at least three fields of view for each well at a particular time point. The experiments were repeated twice with similar results. See also Supplemental Experimental Procedures.

Statistical Analysis

Data were analyzed with Microsoft Excel and KaleidaGraph software. The average values were obtained from several (two to four) independent experiments, and error bars represent SEs of the mean values. Statistical significance was determined by a two-tailed Student's t test (p < 0.05 was considered statistically significant).

REFERENCES

Arnett, E., Lehrer, R.I., Pratikhya, P., Lu, W., and Seveau, S. (2011). Defensins enable macrophages to inhibit the intracellular proliferation of Listeria monocytogenes. Cell. Microbiol. *13*, 635–651.

Arnett, E., Vadia, S., Nackerman, C.C., Oghumu, S., Satoskar, A.R., McLeish, K.R., Uriarte, S.M., and Seveau, S. (2014). The pore-forming toxin listeriolysin O is degraded by neutrophil metalloproteinase-8 and fails to mediate Listeria monocytogenes intracellular survival in neutrophils. J. Immunol. *192*, 234–244.

Barrera, N.P., Di Bartolo, N., Booth, P.J., and Robinson, C.V. (2008). Micelles protect membrane complexes from solution to vacuum. Science *321*, 243–246.

Bokarewa, M., and Tarkowski, A. (2004). Human alpha -defensins neutralize fibrinolytic activity exerted by staphylokinase. Thromb. Haemost. *91*, 991–999.

Castagnini, M., Picchianti, M., Talluri, E., Biagini, M., Del Vecchio, M., Di Procolo, P., Norais, N., Nardi-Dei, V., and Balducci, E. (2012). Arginine-specific mono ADP-ribosylation in vitro of antimicrobial peptides by ADP-ribosylating toxins. PLoS ONE *7*, e41417.

Chu, H., Pazgier, M., Jung, G., Nuccio, S.P., Castillo, P.A., de Jong, M.F., Winter, M.G., Winter, S.E., Wehkamp, J., Shen, B., et al. (2012). Human α-defensin 6 promotes mucosal innate immunity through self-assembled peptide nanonets. Science *337*, 477–481.

Chumbler, N.M., Farrow, M.A., Lapierre, L.A., Franklin, J.L., Haslam, D.B., Goldenring, J.R., and Lacy, D.B. (2012). Clostridium difficile Toxin B causes epithelial cell necrosis through an autoprocessing-independent mechanism. PLoS Pathog. *8*, e1003072.

Conibear, A.C., Rosengren, K.J., Harvey, P.J., and Craik, D.J. (2012). Structural characterization of the cyclic cystine ladder motif of θ-defensins. Biochemistry *51*, 9718–9726.

Cordero, C.L., Kudryashov, D.S., Reisler, E., and Satchell, K.J. (2006). The Actin cross-linking domain of the Vibrio cholerae RTX toxin directly catalyzes the covalent cross-linking of actin. J. Biol. Chem. *281*, 32366–32374.

Demirkhanyan, L.H., Marin, M., Padilla-Parra, S., Zhan, C., Miyauchi, K., Jean-Baptiste, M., Novitskiy, G., Lu, W., and Melikyan, G.B. (2012). Multifaceted mechanisms of HIV-1 entry inhibition by human α-defensin. J. Biol. Chem. *287*, 28821–28838.

Dunstone, M.A., and Tweten, R.K. (2012). Packing a punch: the mechanism of pore formation by cholesterol dependent cytolysins and membrane attack complex/perforin-like proteins. Curr. Opin. Struct. Biol. *22*, 342–349.

Eftink, M.R., and Ghiron, C.A. (1976). Exposure of tryptophanyl residues in proteins. Quantitative determination by fluorescence quenching studies. Biochemistry *15*, 672–680.

Feld, G.K., Brown, M.J., and Krantz, B.A. (2012). Ratcheting up protein translocation with anthrax toxin. Protein Sci. *21*, 606–624.

Flatt, J.W., Kim, R., Smith, J.G., Nemerow, G.R., and Stewart, P.L. (2013). An intrinsically disordered region of the adenovirus capsid is implicated in neutralization by human alpha defensin 5. PLoS ONE *8*, e61571.

Fontana, A., de Laureto, P.P., Spolaore, B., Frare, E., Picotti, P., and Zambonin, M. (2004). Probing protein structure by limited proteolysis. Acta Biochim. Pol. *51*, 299–321.

Furci, L., Sironi, F., Tolazzi, M., Vassena, L., and Lusso, P. (2007). Alpha-defensins block the early steps of HIV-1 infection: interference with the binding of gp120 to CD4. Blood *109*, 2928–2935.

Giesemann, T., Guttenberg, G., and Aktories, K. (2008). Human alpha-defensins inhibit Clostridium difficile toxin B. Gastroenterology *134*, 2049–2058.

Glomski, I.J., Gedde, M.M., Tsang, A.W., Swanson, J.A., and Portnoy, D.A. (2002). The Listeria monocytogenes hemolysin has an acidic pH optimum to compartmentalize activity and prevent damage to infected host cells. J. Cell Biol. *156*, 1029–1038.

Gounder, A.P., Wiens, M.E., Wilson, S.S., Lu, W., and Smith, J.G. (2012). Critical determinants of human α-defensin 5 activity against non-enveloped viruses. J. Biol. Chem. *287*, 24554–24562.

Hawkins, M., Pope, B., Maciver, S.K., and Weeds, A.G. (1993). Human actin depolymerizing factor mediates a pH-sensitive destruction of actin filaments. Biochemistry *32*, 9985–9993.

Hooven, T.A., Randis, T.M., Hymes, S.R., Rampersaud, R., and Ratner, A.J. (2012). Retrocyclin inhibits Gardnerella vaginalis biofilm formation and toxin activity. J. Antimicrob. Chemother. *67*, 2870–2872.

Hsu, W.L., Oldfield, C., Meng, J., Huang, F., Xue, B., Uversky, V.N., Romero, P., and Dunker, A.K. (2012). Intrinsic protein disorder and protein-protein interactions. Pac. Symp. Biocomput. *2012*, 116–127.

Kim, C., Gajendran, N., Mittrücker, H.W., Weiwad, M., Song, Y.H., Hurwitz, R., Wilmanns, M., Fischer, G., and Kaufmann, S.H. (2005). Human alpha-defensins neutralize anthrax lethal toxin and protect against its fatal consequences. Proc. Natl. Acad. Sci. USA *102*, 4830–4835.

Kim, C., Slavinskaya, Z., Merrill, A.R., and Kaufmann, S.H. (2006). Human alpha-defensins neutralize toxins of the mono-ADP-ribosyltransferase family. Biochem. J. *399*, 225–229.

Kohlgraf, K.G., Pingel, L.C., Dietrich, D.E., and Brogden, K.A. (2010). Defensins as anti-inflammatory compounds and mucosal adjuvants. Future Microbiol. *5*, 99–113.

Kudryashov, D.S., Durer, Z.A., Ytterberg, A.J., Sawaya, M.R., Pashkov, I., Prochazkova, K., Yeates, T.O., Loo, R.R., Loo, J.A., Satchell, K.J., and Reisler, E. (2008). Connecting actin monomers by iso-peptide bond is a toxicity mechanism of the Vibrio cholerae MARTX toxin. Proc. Natl. Acad. Sci. USA *105*, 18537–18542.

Kudryashova, E., Kalda, C., and Kudryashov, D.S. (2012). Glutamyl phosphate is an activated intermediate in actin crosslinking by actin crosslinking domain (ACD) toxin. PLoS ONE *7*, e45721.

Kudryashova, E., Heisler, D., Zywiec, A., and Kudryashov, D.S. (2014). Thermodynamic properties of the effector domains of MARTX toxins suggest their unfolding for translocation across the host membrane. Mol. Microbiol. *92*, 1056–1071. http://dx.doi.org/10.1111/mmi.12615.

Lehrer, R.I., Jung, G., Ruchala, P., Wang, W., Micewicz, E.D., Waring, A.J., Gillespie, E.J., Bradley, K.A., Ratner, A.J., Rest, R.F., and Lu, W. (2009). Human alpha-defensins inhibit hemolysis mediated by cholesterol-dependent cytolysins. Infect. Immun. *77*, 4028–4040.

Lyon, A.N., Pineda, R.H., Hao, T., Kudryashova, E., Kudryashov, D.S., and Beattie, C.E. (2014). Calcium binding is essential for plastin 3 function in Smn-deficient motoneurons. Hum. Mol. Genet. *23*, 1990–2004.

Madison, M.N., Kleshchenko, Y.Y., Nde, P.N., Simmons, K.J., Lima, M.F., and Villalta, F. (2007). Human defensin alpha-1 causes Trypanosoma cruzi membrane pore formation and induces DNA fragmentation, which leads to trypanosome destruction. Infect. Immun. *75*, 4780–4791.

Marriott, H.M., Mitchell, T.J., and Dockrell, D.H. (2008). Pneumolysin: a double-edged sword during the host-pathogen interaction. Curr. Mol. Med. *8*, 497–509.

Montagner, C., Perier, A., Pichard, S., Vernier, G., Ménez, A., Gillet, D., Forge, V., and Chenal, A. (2007). Behavior of the N-terminal helices of the diphtheria toxin T domain during the successive steps of membrane interaction. Biochemistry *46*, 1878–1887.

Niu, S., Rabuck, J.N., and Ruotolo, B.T. (2013). Ion mobility-mass spectrometry of intact protein—ligand complexes for pharmaceutical drug discovery and development. Curr. Opin. Chem. Biol. *17*, 809–817.

Panyutich, A.V., Panyutich, E.A., Krapivin, V.A., Baturevich, E.A., and Ganz, T. (1993). Plasma defensin concentrations are elevated in patients with septicemia or bacterial meningitis. J. Lab. Clin. Med. *122*, 202–207.

Prochazkova, K., Shuvalova, L.A., Minasov, G., Voburka, Z., Anderson, W.F., and Satchell, K.J. (2009). Structural and molecular mechanism for autoprocessing of MARTX toxin of Vibrio cholerae at multiple sites. J. Biol. Chem. *284*, 26557–26568.

Satchell, K.J. (2011). Structure and function of MARTX toxins and other large repetitive RTX proteins. Annu. Rev. Microbiol. *65*, 71–90.

Senisterra, G.A., and Finerty, P.J., Jr. (2009). High throughput methods of assessing protein stability and aggregation. Mol. Biosyst. *5*, 217–223.

Seveau, S. (2014). Multifaceted activity of listeriolysin O, the cholesterol-dependent cytolysin of Listeria monocytogenes. Subcell. Biochem. *80*, 161–195.

Shen, A., Lupardus, P.J., Albrow, V.E., Guzzetta, A., Powers, J.C., Garcia, K.C., and Bogyo, M. (2009). Mechanistic and structural insights into the proteolytic activation of Vibrio cholerae MARTX toxin. Nat. Chem. Biol. *5*, 469–478.

Spudich, J.A., and Watt, S. (1971). The regulation of rabbit skeletal muscle contraction. I. Biochemical studies of the interaction of the tropomyosin-troponin complex with actin and the proteolytic fragments of myosin. J. Biol. Chem. *246*, 4866–4871.

Thoren, K.L., and Krantz, B.A. (2011). The unfolding story of anthrax toxin translocation. Mol. Microbiol. *80*, 588–595.

Tokuriki, N., Oldfield, C.J., Uversky, V.N., Berezovsky, I.N., and Tawfik, D.S. (2009). Do viral proteins possess unique biophysical features? Trends Biochem. Sci. *34*, 53–59.

Vega, L.A., and Caparon, M.G. (2012). Cationic antimicrobial peptides disrupt the Streptococcus pyogenes ExPortal. Mol. Microbiol. *85*, 1119–1132.

Wei, G., Pazgier, M., de Leeuw, E., Rajabi, M., Li, J., Zou, G., Jung, G., Yuan, W., Lu, W.Y., Lehrer, R.I., and Lu, W. (2010). Trp-26 imparts functional versatility to human alpha-defensin HNP1. J. Biol. Chem. *285*, 16275–16285.

Wesche, J., Elliott, J.L., Falnes, P.O., Olsnes, S., and Collier, R.J. (1998). Characterization of membrane translocation by anthrax protective antigen. Biochemistry *37*, 15737–15746.

Wilson, S.S., Wiens, M.E., and Smith, J.G. (2013). Antiviral mechanisms of human defensins. J. Mol. Biol. *425*, 4965–4980.

Wu, Z., Hoover, D.M., Yang, D., Boulègue, C., Santamaria, F., Oppenheim, J.J., Lubkowski, J., and Lu, W. (2003a). Engineering disulfide bridges to dissect antimicrobial and chemotactic activities of human beta-defensin 3. Proc. Natl. Acad. Sci. USA *100*, 8880–8885.

Wu, Z., Powell, R., and Lu, W. (2003b). Productive folding of human neutrophil alpha-defensins in vitro without the pro-peptide. J. Am. Chem. Soc. *125*, 2402–2403.

Wu, Z., Ericksen, B., Tucker, K., Lubkowski, J., and Lu, W. (2004). Synthesis and characterization of human alpha-defensins 4-6. J. Pept. Res. *64*, 118–125.

Wylie, C.S., and Shakhnovich, E.I. (2011). A biophysical protein folding model accounts for most mutational fitness effects in viruses. Proc. Natl. Acad. Sci. USA *108*, 9916–9921.

Yin, S., Xie, Y., and Loo, J.A. (2008). Mass spectrometry of protein-ligand complexes: enhanced gas-phase stability of ribonuclease-nucleotide complexes. J. Am. Soc. Mass Spectrom. *19*, 1199–1208.

Zhang, Y., Lu, W., and Hong, M. (2010). The membrane-bound structure and topology of a human α-defensin indicate a dimer pore mechanism for membrane disruption. Biochemistry *49*, 9770–9782.

Zhao, L., and Lu, W. (2014). Defensins in innate immunity. Curr. Opin. Hematol. *21*, 37–42.

Zhao, L., Ericksen, B., Wu, X., Zhan, C., Yuan, W., Li, X., Pazgier, M., and Lu, W. (2012). Invariant gly residue is important for α-defensin folding, dimerization, and function: a case study of the human neutrophil α-defensin HNP1. J. Biol. Chem. *287*, 18900–18912.

Zhao, L., Tolbert, W.D., Ericksen, B., Zhan, C., Wu, X., Yuan, W., Li, X., Pazgier, M., and Lu, W. (2013). Single, double and quadruple alanine substitutions at oligomeric interfaces identify hydrophobicity as the key determinant of human neutrophil alpha defensin HNP1 function. PLoS ONE *8*, e78937.

Zhou, M., Dagan, S., and Wysocki, V.H. (2012). Protein subunits released by surface collisions of noncovalent complexes: nativelike compact structures revealed by ion mobility mass spectrometry. Angew. Chem. Int. Ed. Engl. *51*, 4336–4339.